High-performance time-resolved fluorescence by direct waveform recording

Joseph M. Muretta,[1] Alexander Kyrychenko,[3] Alexey S. Ladokhin,[3] David J. Kast,[1] Gregory D. Gillispie,[2] and David D. Thomas[1,a)]
[1]*Department of Biochemistry, Molecular Biology and Biophysics, University of Minnesota, Minneapolis, Minnesota 55455, USA*
[2]*Fluorescence Innovations, Inc., Bozeman, Montana 59718, USA*
[3]*Department of Biochemistry and Molecular Biology, University of Kansas Medical Center, Kansas City, Kansas 66160, USA*

(Received 20 April 2010; accepted 26 July 2010; published online 15 October 2010)

We describe a high-performance time-resolved fluorescence (HPTRF) spectrometer that dramatically increases the rate at which precise and accurate subnanosecond-resolved fluorescence emission waveforms can be acquired in response to pulsed excitation. The key features of this instrument are an intense (1 μJ/pulse), high-repetition rate (10 kHz), and short (1 ns full width at half maximum) laser excitation source and a transient digitizer (0.125 ns per time point) that records a complete and accurate fluorescence decay curve for every laser pulse. For a typical fluorescent sample containing a few nanomoles of dye, a waveform with a signal/noise of about 100 can be acquired in response to a single laser pulse every 0.1 ms, at least 10^5 times faster than the conventional method of time-correlated single photon counting, with equal accuracy and precision in lifetime determination for lifetimes as short as 100 ps. Using standard single-lifetime samples, the detected signals are extremely reproducible, with waveform precision and linearity to within 1% error for single-pulse experiments. Waveforms acquired in 0.1 s (1000 pulses) with the HPTRF instrument were of sufficient precision to analyze two samples having different lifetimes, resolving minor components with high accuracy with respect to both lifetime and mole fraction. The instrument makes possible a new class of high-throughput time-resolved fluorescence experiments that should be especially powerful for biological applications, including transient kinetics, multidimensional fluorescence, and microplate formats. © *2010 American Institute of Physics.*
[doi:10.1063/1.3480647]

I. INTRODUCTION

A wide scope of applications in biological research and biotechnology rely on the high intrinsic sensitivity and environmental dependence of fluorescence signals. Fluorescence excitation and emission spectra, the excited-state lifetime, polarization, and quantum yield can be extremely sensitive to changes in temperature, solvent polarity, viscosity, dynamics, and proximity to other chromophores or quenchers. Diverse methods are available for measuring fluorescence signals. In general, these methods can be classified into two types of experiment: steady-state (SS) and time-resolved (TR) fluorescence. In SS fluorescence, the sample is continuously excited and detected with the ensemble of fluorophores maintained in a photophysical steady state. Most fluorescence measurements involve SS methods, primarily because SS data can be acquired very rapidly, allowing high-throughput data acquisition. However, the SS fluorescence of a typical fluorophore has insufficient spectral resolution to resolve two or more different photophysical states. A SS measurement usually yields a single intensity number that reflects a global ensemble average of photophysical states in the sample, without resolving them. In contrast, TR fluorescence, in which the emission waveform is detected as a function of time after a brief excitation pulse, is exquisitely sensitive to the nonradiative decay processes that arise from variations in the molecular structure, dynamics, and environment of the fluorophore. The individual exponential lifetime components of a time-resolved fluorescence decay correspond to specific photophysical states of the fluorophore, and these lifetimes often resolve distinct structural or chemical states of the fluorescent dye and its attached macromolecule, while the corresponding preexponential amplitudes define the mole fractions (thermodynamics) of the associated states. The extra dimensionality of TR fluorescence allows direct analysis of complex structure and thermodynamics in a single measurement.

Time-correlated single-photon counting (TCSPC), which is the most widely practiced form of TR fluorescence, does not provide high-throughput capability. TCSPC detects TR fluorescence by measuring the time for the first emitted photon to reach the detector, following a brief excitation pulse. Repeating this measurement many times produces a histogram of detected "first photons." The histogram is a faithful representation of the true fluorescence waveform of the sample, provided that the sample was stable during the

a)Author to whom correspondence should be addressed. Electronic mail: ddt@umn.edu.

course of the measurement and that no more than an average of one photon is counted per 100 excitation pulses.[1] Photon counting follows Poisson statistics, so the measured signal/noise (S/N) is no greater than the square root of the number of photons in the peak channel. To obtain $S/N=100$, a minimum for reliable analysis of multiexponential fluorescence decays, requires collecting data until $\sim 10^4$ photons have accumulated in the peak channel.[2] This corresponds to $\sim 10^6$ total photons (thus 10^8 pulses), assuming a 10 ns lifetime and 1000 channels, 0.1 ns each. With a pulsed laser operating at optimum repetition frequency ($(10^*\tau)^{-1} \approx 10^7$ s^{-1}), it takes at least 10 s to generate the required 10^8 pulses, yielding a single TR fluorescence waveform with $S/N \sim 100$. Thus, the TCSPC acquisition is slow compared to SS and cannot be used to analyze transient changes in a sample that occur faster than tens of seconds. It is not suited for high-throughput applications such as screening large arrays of samples where the measurement is repeated thousands of times. Stroboscopic[3] and frequency-domain methods[1] do detect photons at a higher rate, but they require scanning of either a time window or frequency, thus prolonging data acquisition to the time scale of seconds.

The only realistic possibility for acquiring high-throughput TR data is direct waveform recording (DWR), in which the entire time course of the TR emission waveform is detected after a single excitation pulse, using a fast transient analog-to-digital converter. A huge advantage in data throughput results when thousands of photons are detected per pulse, instead of 1 photon every 100 pulses. At first glance, this seems quite feasible; for decades, there have been subnanosecond pulsed lasers capable of exciting strong fluorescence signals, and transient digitizers with subnanosecond resolution. Indeed, there have been reports of direct waveform recording of time-resolved fluorescence signals for decades, based on detection with streak cameras,[4] digital oscilloscopes,[5] or other transient digitizers.[6] However, these methods have been plagued by systematic errors and have thus not been shown to approach the precision or accuracy of the TCSPC method.[1] The utility of DWR in quantitative analysis of time-resolved fluorescence on a high-throughput basis has been severely limited by the requirement that the digital signal must be accurate (linearly amplified and detected) and highly reproducible, since data analysis requires the precise comparison of the TR waveform with the experimentally-acquired instrument-response function (IRF). The IRF is used in a reconvolution procedure to recover the effective response of the sample to a delta function pulse. While fast fluorescence signals from single laser pulses have been reported with apparently high S/N, their accuracy and reproducibility has been insufficient for reliable quantitative analysis of exponential and multiexponential decays.[7]

In the present study, we describe an instrument in which these criteria have been met to a level that yields time-resolved fluorescence waveforms that have precision to better than 1% and accuracy to better than 0.5%, with reproducible acquisition of the entire waveform every 0.1 ms. We accomplished this by using a 10 kHz passively Q-switched microchip laser with extremely reproducible pulses that are sufficiently energetic (~ 1 μJ) and narrow (~ 1 ns) for nanosecond scale fluorescence lifetime measurements, and a transient digitizer with 0.125 ns resolution and high linearity. We tested this instrument using well-characterized fluorescent dyes in the micromolar concentration range, showing that a single-pulse experiment, complete in 0.1 ms, provides information equivalent to that of a optimized TCSPC experiment, performed on an identical sample, lasting 1 min (at least 10^5 times longer). We show that the instrument is capable of resolving two-component dye systems with high precision, producing accurate values for both lifetimes and mole fractions. The experiment performed by this instrument is designated *high-performance time-resolved fluorescence* (HPTRF) to indicate its unique combination of precision, accuracy, and high-throughput data acquisition. This advancement will allow a new class of experiments to be performed, in which accurate high-resolution TR fluorescence is acquired in a high-throughput platform.

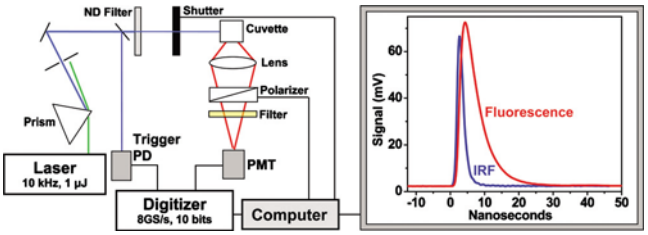

FIG. 1. (Color) Left: schematic diagram of HPTRF instrument, as described in text. Right: typical acquired data, showing the average of 1000 pulses (total acquisition time 0.1 s) for the IRF (light scatter from glycogen in water) and fluorescence (5 μM anthracene in MeOH). Acquisition is triggered at t=−12.5 ns by a signal from a photodiode, and excitation begins at t=0.

II. METHODS

A. Instrument design

A schematic representation of the HPTRF instrument and the format of acquired data are given in Fig. 1. The excitation source is a microchip diode-pumped yttrium aluminum garnet laser (NanoUV-355, JDS Uniphase), optimized to operate at the third harmonic (355 nm). At our request, the laser was delivered without harmonic separation optics, thereby providing access to the second harmonic (532 nm). The desired harmonic was selected with a dispersing prism. The mechanism of pulse generation in passively Q-switched lasers such as this avoids electromagnetic noise that can interfere with the detection electronics. This laser continuously generates narrow [<1 ns full width at half maximum (FWHM)] pulses that are extremely uniform in shape and intensity, at a 10 kHz repetition frequency. The pulse energy available for excitation is about 1 μJ at both 532 and 355 nm, which is enough to excite billions of molecules in a typical fluorescent sample. Sample solutions were contained in a standard water-jacketed 1 cm quartz cuvet, and temperature was controlled by a recirculating water bath. The emission polarizer was usually set at the magic angle (54.7° relative to the vertical excitation). Unless otherwise indicated, the emission wavelength was selected by an interference filter, but a monochromator (Varian Cary Eclipse) was also available. Emission was focused into the

photomultiplier tube (PMT) (PMT in Fig. 1) module (H5773-20, Hamamatsu), which was chosen because of its 0.78 ns rise time and 300–900 nm spectral range. The anode current from the PMT was input to a fast digitizer (Acqiris DC252) with 10-bit amplitude resolution (full range set at 100 mV in this study), maximum time resolution 8×10^9 points/s (0.125 ns/point), maximum recording rate 500 000 waveforms/s, and maximum storage 125 000 waveforms and 1×10^9 points. To maximize sensitivity and precision for a given sample, we maximized the number of photons detected with each excitation pulse, using the minimum amplification (PMT high voltage) needed to produce a full-scale signal at the digitizer. To achieve this, the maximum signal was adjusted to be in the range of 50–80 mV by first decreasing the PMT high voltage (450–800 V) with no attenuation of the laser, then (as necessary) attenuating the laser with a neutral density filter or wave plate. To minimize photobleaching, a computer-controlled shutter remained closed except during data acquisition. Photobleaching was typically found to be negligible during a 1000-pulse acquisition.

Waveform recording by the digitizer is initiated by a trigger signal from a photodiode (PD) (PD in Fig. 1), which is fed by a fiber-optic cable positioned to pick up a portion of the laser beam. There is a delay, typically set at 12.5 ns, precisely fixed by the acquisition software, between the trigger and the excitation pulse (Fig. 1, right). Because the digitizer is not synchronized to the pulsed laser, the position of the pulse varies randomly across the 0.125 ns channel width, producing a uniform distribution of time shifts for the detected waveform. The signal averaging of 1000 waveforms reduces the effective width of this time uncertainty to ~2 ps. For each set of fluorescence experiments (Fig. 1, red waveform), the instrument response function (IRF) (IRF, blue waveform in Fig. 1) was acquired under identical conditions, except that the cuvet contained water and enough latex microspheres (Nanospheres, 20 nm diameter, Thermo Scientific, Fremont, CA) to give a full-range (50–80 mV) signal, the emission polarization was set at vertical (0°), and the emission filter was removed to detect scattered light.[8] The IRF waveform, which typically showed about 1.5 ns full width at half maximum depending on the exact PMT voltage of each acquisition, was used in data analysis as described below.

Data acquisition was accomplished using a computer program that controls digitizer parameters such as amplitude scale and sampling frequency, as well as data transfer, averaging, and visualization. Digitizer memory was divided into segments, each of which contained a single-pulse time-resolved waveform record with 500 data points, corresponding to a 62.5-ns time base (Fig. 1, right). The acquisition software allows single-pulse waveforms to be recorded for up to 12.5 s (125 000 pulses) before transfer to the control computer for storage, signal averaging, and analysis. Each waveform record includes at least 100 points of prepulse data, which is used to calculate the background during data analysis.

In selected cases, waveforms were acquired by the TCSPC method[9] from identical samples, using the same optical components and light path. This instrument used state-of-the-art components, including a subnanosecond pulsed diode laser (PicoQuant LDH 375), operating at an optimal repetition rate of 10 MHz and a wavelength of 375 nm, a PMH-100 photomultiplier module, and a SPC-130-EM photon-counting board (Becker-Hickl, Berlin, Germany). The fluorescence waveform was recorded within 1024 channels, at 58 ps/channel. Each waveform was typically acquired until a peak value of 10 000 counts was obtained, in order to obtain $S/N\sim100$ in the peak channel. The instrumental response function (IRF) was recorded as described above, yielding a waveform with 0.3 ns full width at half maximum. Some measurements were also performed with a commercial instrument (FluoTime 200, PicoQuant, Berlin, Germany) at the University of Kansas.[9]

B. Samples

We analyzed five dyes that are known to have single-exponential decay kinetics, anthracene (Anth), 9,10-dibromoanthracene (DBA), rhodamine-6-G (Rh6G), rhodamine-B (RhB), and Rose Bengal (RB). The anthracenes were excited at 355 or 373 nm (thus allowing a direct comparison between HPTRF and TCSPC), while Rh6G, RhB, and RB were excited at 532 nm. The mixtures of Anth and DBA or Rh6G and RhB were used in experiments testing the ability to resolve multiple fluorescent components. RB was chosen to test the sensitivity to subnanosecond lifetimes. Dyes were dissolved in double distilled water (Rh6G, RhB, and RB) or in spectroscopic grade methanol (Anth, DBA). All solvents are equilibrated with ambient air. The experiments were performed at 25 °C.

C. Data analysis

Background was calculated for each waveform by computing the mean of the first 100 pretrigger data points and this value was subtracted from the waveform prior to analysis. For a comparison of waveform shapes, normalization was performed by dividing the waveform by its integral. All data were plotted using Origin 8. Fluorescence lifetimes were analyzed using a custom-built software platform (FARGOFIT, written by Igor Negrashov) designed for the global analysis of TR fluorescence. The observed waveform $F_{obs}(t)$ was fitted with a simulation $F_{sim}(t)$, consisting of a multiexponential decay $F(t)$ convolved with the measured instrument response function (IRF),

$$F(\mathrm{t}) = \sum_{i=1}^{n} A_\mathrm{i} \exp(-t/\tau_\mathrm{i}),$$

$$F_{sim}(t) = \int_{-\infty}^{+\infty} \mathrm{IRF}(t-t')F(t'+q)dt', \tag{1}$$

where A_i are amplitudes (proportional to mol fractions), τ_i are fluorescence lifetimes, and q is a time shift applied to align the IRF with the fluorescence decay. These $2n+1$ parameters were determined by minimizing χ^2 between F_{sim} and F_{obs}, using either Marquardt or Simplex optimization algorithms. The number of components n was determined as

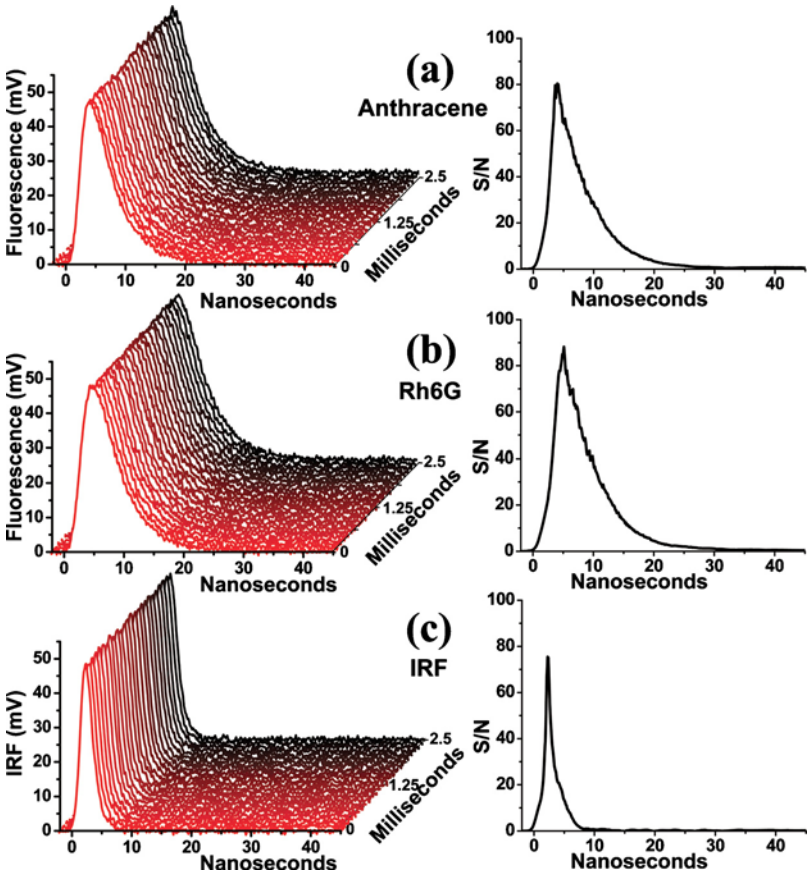

FIG. 2. (Color online) Waveform precision of HPTRF. Left: the first 25 of the 1000 single-pulse waveforms acquired every 0.1 ms. Right: S/N, where S(t) is the mean signal intensity, and N(t) is the standard deviation, calculated for all 1000 waveforms. (a) 5 μM anthracene in methanol. (b) 1 μM rhodamine 6G in water. (c) IRF.

the minimum value that significantly decreased χ^2. Analysis was performed on individual waveforms or globally on collections of waveforms. For global analysis, one or more parameters from $F(t)$ were assumed to be the same for all waveforms.[10,11] Uncertainty of determined parameters was estimated from the standard error of the mean of independently analyzed replicate data sets. Precision of a single determination was estimated from the standard deviation.

III. EXPERIMENTAL RESULTS

A. Precision of single-pulse waveforms

The precision of HPTRF measurements was determined from sets of 1000 single-pulse waveforms using a standard sample of 5 μM anthracene in methanol [Fig. 2(a)] or 1 μM rhodamine 6G in water [Fig. 2(b)]. Each waveform was acquired from a single excitation pulse, so each 1000-pulse data set was acquired in a total of 0.1 s. IRF waveforms were acquired using the same protocol [Fig. 2(c)]. Repeated single-pulse waveforms exhibit remarkably small variation in intensity or shape. S/N was calculated as mean/SD (Fig. 2, right), giving peak S/N values of 80 for 5 μM anthracene [Fig. 2(a)], 88 for 1 μM Rh6G [Fig. 2(b)], and 75 for IRF [Fig. 2(c)]. Of course, further improvement in S/N is achieved by signal averaging, as discussed below or by increasing dye concentration. Lifetimes determined from these single-pulse waveforms were also quite precise, exhibiting SD values less than 1%.

B. Signal detection linearity

Accurate analysis of a complex fluorescent sample requires that the intensity of the detected waveform depends linearly on the excitation intensity, without changing the shape of the waveform. To test this, we acquired waveforms from Rh6G and RB over an order of magnitude of excitation intensities, resulting in signal amplitudes that varied from about 5 to 50 mV [Fig. 3(a)]. The intensity of the excitation pulse was varied by rotating a waveplate, aligned in the excitation path, such that each successive rotation decreased the excitation pulse intensity by precisely 10% increments. The total integrated fluorescence for both samples increased linearly with excitation intensity [Fig. 3(b)]. When the waveforms were normalized to their peak intensities and overlaid, they were indistinguishable [Fig. 3(c)], with standard deviations less than 0.5% [Fig. 3(d)], showing that the intensities and shapes of acquired waveforms are linear to 0.5% over a tenfold range of signal intensities.

C. Comparison of HPTRF with TCSPC

We acquired the TR-fluorescence waveform of the same 5 μM anthracene sample by both HPTRF and TCSPC (Fig. 4). To ensure accurate and reproducible comparisons of lifetime and system performance, a diode laser and TCSPC detection system were incorporated into the HPTRF optical path, as described in Sec. II. Figure 4 shows that the waveform acquired from a single-pulse HPTRF experiment is essentially equivalent in lifetime (top) and S/N (bottom) to a waveform acquired by TCSPC in 60 s. For HPTRF, a single-

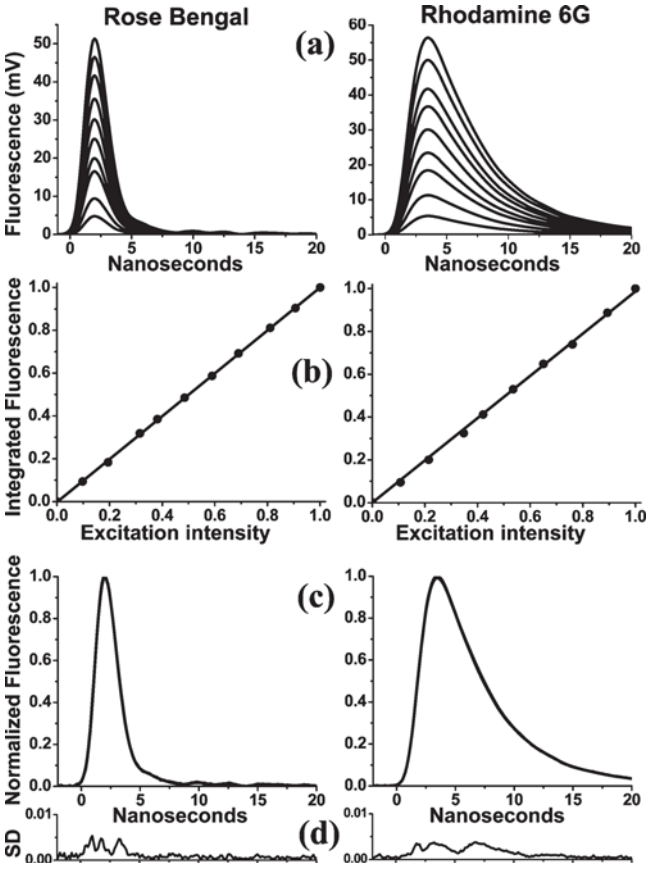

FIG. 3. Linearity of waveforms. (a) Waveforms, averaged from 1000 pulses (100 ms total acquisition time), are recorded for 1 μM RB (left) and 1 μM Rh6G (right) with variable excitation intensity. (b) Integrated fluorescence vs excitation intensity. (c) Waveforms from (a) normalized by values in (b). All ten waveforms are plotted and overlaid, showing excellent reproducibility. (d) Standard deviations from (c).

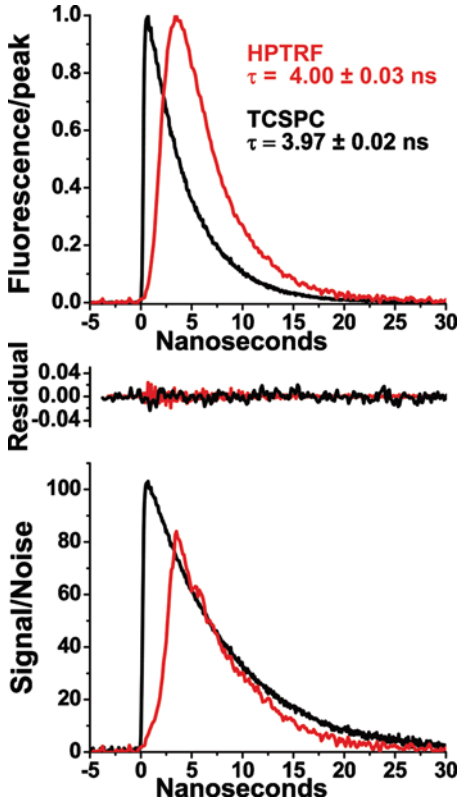

FIG. 4. (Color) Fluorescence waveforms acquired from 5 μM anthracene by HPTRF (red, acquired from a single pulse) and TCSPC (black, 60 s acquisition time). Residuals are from single-exponential fits. Lifetime values are given as mean and standard deviation from repeated acquisitions. Signal/Noise=S(t)/N(t), where S(t) is the background-subtracted signal of a single-pulse HPTRF acquisition or a 60-s TCSPC acquisition and N(t) is the standard deviation, calculated for 1000 replicate acquisitions (HPTRF) or $S(t)^{1/2}$ (TCSPC).

pulse waveform was acquired every 0.1 ms, resulting in a peak S/N ~ 80 for each individual waveform. For TCSPC, 10 000 counts (resulting from 6×10^8 pulses) were accumulated in the peak channel in 60 s total data acquisition time, resulting in a peak S/N ~ 100. Thus the time needed to obtain equivalent S/N is about 6×10^5 times longer for TCSPC than for HPTRF. We analyzed the fluorescence decays by identical procedures, fitting with multiexponential functions convolved with the IRF from each instrument [Eq. (1), Fig. 4]. Both data sets were best fit by a single-exponential model [n=1 in Eq. (1)]; two exponentials did not improve the fit. While the TCSPC waveform rises and decays faster, due to its narrower IRF, the two lifetimes determined were essentially identical in both mean and SD (HPTRF $\tau=4.00\pm0.03$ ns, TCSPC $\tau=3.97\pm0.02$ ns, Fig. 4). The residuals from both fits were similar, approximately 1% of peak intensity (Fig. 4, middle). TCSPC measurements were also performed on a commercially available instrument in the laboratory of ASL at the University of Kansas Medical Center, using similar experimental conditions.[9] The results from these experiments were essentially identical ($\tau=4.05\pm0.04$ ns) to those obtained with the HPTRF instrument and with the TCSPC system (Fig. 4).

D. Lifetime measurement for standard dyes

The fluorescence lifetimes of several standard dyes were measured, excited either at 355 nm [Fig. 5(a)] or 532 nm [Fig. 5(b)]. Each data set was recorded as the average of 1000 waveforms, resulting in a total acquisition time of 0.1 s. All five dyes were best fit by a single exponential model [Eq. (1), n=1]. The measured lifetimes were in excellent agreement with published literature values (Table I).

A small (<0.5% of peak amplitude) nonrandom pattern is observed in the residuals (Fig. 5), probably due to slight

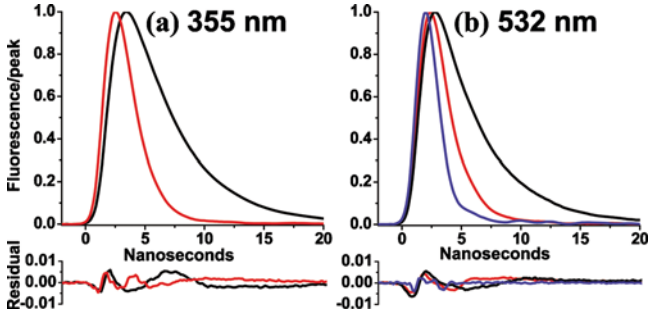

FIG. 5. (Color) Lifetime analysis of standard dyes excited at (a) 355 nm (5 nM DBA black, Anth red) and (b) 532 nm (1 μM RB blue, RB red, Rh6G black,) and analyzed using FARGOFIT. Residuals are from single exponential fits. Lifetimes are in Table I.

TABLE I. Lifetimes (nanosecond) of fluorescent standards. (Mean ± SEM of 5–8 trials.)

Dye	Solvent	This study	Literature
Anthracene	MeOH	4.05 ± 0.02	4.09 ± 0.05 [a]
Dibromoanthracene	MeOH	1.20 ± 0.04	1.18 ± 0.20 [b]
Rhodamine-6-G	Water	4.00 ± 0.01	4.08 ± 0.08 [c]
Rhodamine B	Water	1.62 ± 0.02	1.74 ± 0.02 [d]
Rose Bengal	Water	0.10 ± 0.02	0.12 ± 0.02 [e]

[a]Reference 12.
[b]Reference 13.
[c]Reference 14.
[d]Reference 15.
[e]Reference 16.

nonlinearities in the detection system. However, these small errors are inconsequential, in the sense that they do not interfere significantly with quantitative data analysis, as demonstrated here and below. For example, for single-exponential dyes, these residuals are not affected by incorporating additional decay terms in the model or representing the decay as a Gaussian distribution of lifetimes. When excitation intensity is varied by a factor of 10 as in Fig. 3, the measured lifetime [τ in Eq. (1)] is constant to within 2%, and the measured amplitude [A in Eq. (1)] varies linearly with excitation intensity within 2% (Fig. 6).

E. Analysis of dye mixtures

Experimentally interesting fluorescence samples are typically complex mixtures of fluorescence species having distinct lifetimes, e.g, multiexponential single fluorophores such as tryptophan, mixtures of different fluorophores, or mixtures of conformational states of a labeled macromolecule. A major motivation for performing TR fluorescence is to resolve and quantitate these distinct species, with accurate determination of both lifetimes (containing information about structure or environment) and amplitudes (containing information about thermodynamics or kinetics). To determine whether HPTRF is capable of accurate resolution of distinct species, we analyzed samples containing varied mole fractions of two single-exponential dyes (Fig. 7). Each waveform [Fig. 7(a)], the average of 1000 single-pulse waveforms, was fit to a multiexponential model [Eq. (1)]. In all cases, the double-exponential model was the best fit, since χ^2 improved when n was increased from 1 to 2, but not from 2 to 3. Measured amplitudes A_i were converted to mole fractions using the relative measured signal amplitudes of pure dyes. The analysis accurately (within 0.2 ns for lifetimes or 0.01 for mole fractions) measured the known lifetimes [Fig. 7(b), compare with Table I] and mole fractions [Fig. 7(c)] of the dyes in both mixtures, whether the waveforms were analyzed individually and independently, allowing all amplitudes and lifetimes to vary in Eq. (1) (open circles) or globally, assuming that the same two lifetimes were present in all samples [horizontal lines in Fig. 7(b), closed circles in Fig. 7(c)]. Thus HPTRF has the required accuracy to resolve and quantitate signals from two-component signals.

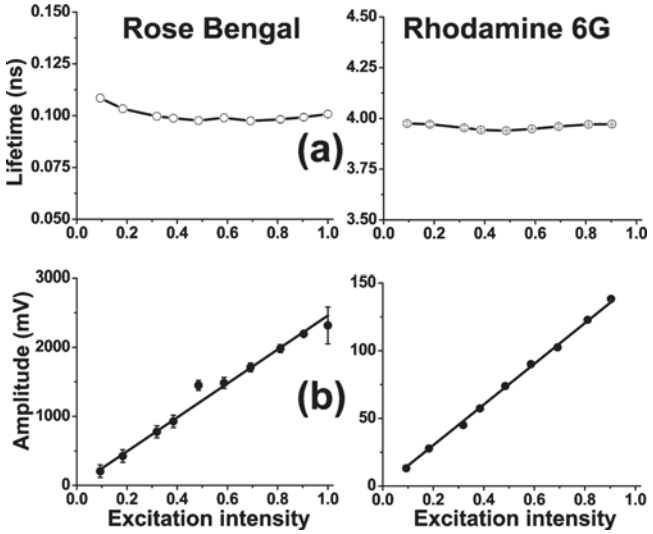

FIG. 6. Fluorescence lifetimes (a) and amplitudes (b) are accurately determined by fitting waveforms to Eq. (1) over a wide range of signal intensity, which was varied by varying excitation intensity as in Fig. 3.

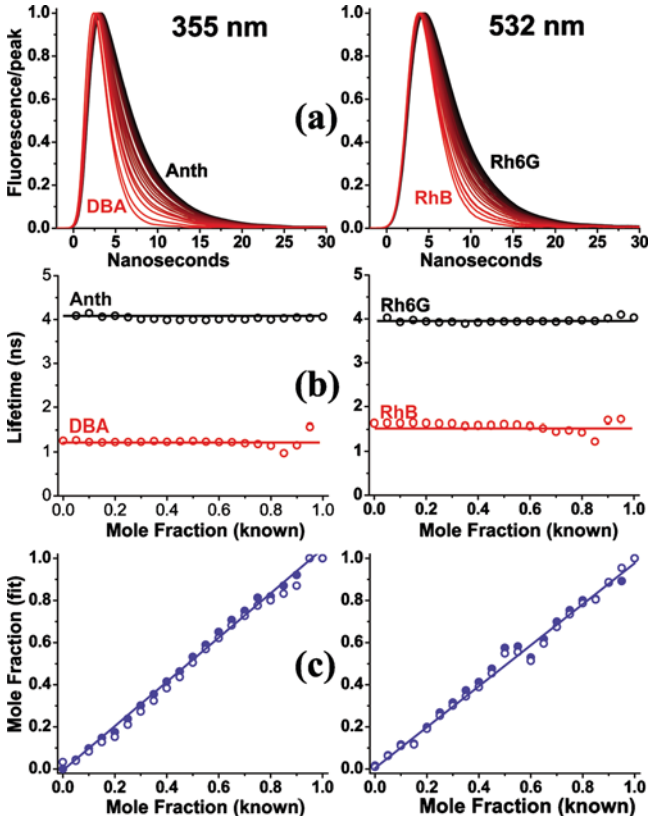

FIG. 7. (Color) Analysis of dye mixtures. Left: dyes excited at 355 nm (Anth and DBA, total concentration 5 μM in methanol). Right: dyes excited at 532 nm (Rh6G and RhB, total concentration 1 μM in water). (a) Each waveform is the average of 1000 single-pulse waveforms, with the mole fraction of the short-lifetime dye increasing from 0 (black) to 1 (red) in 0.05 increments. (b) Lifetimes determined from independent fits (open circles) and from global fits (horizontal lines). (c) Mole fractions of the short-lifetime dye from the same fits as in (b) for independent (open circles) and global (closed circles) analysis.

IV. DISCUSSION

A. Instrument performance

The HPTRF instrument uses direct recording to acquire single-pulse fluorescence waveforms with extremely high precision (Fig. 2) and linearity (Fig. 3), with S/N ~ 100

(Fig. 2) and a lifetime measurement with SD of 1% (Fig. 4) at a repetition rate of 10^4 s^{-1}, about 10^5 times the maximum rate achievable with the conventional TCSPC method (Fig. 4). Lifetimes (as short as 100 ps) and amplitudes are determined accurately (Figs. 4 and 5, Table I) over a wide range of signal intensities (Fig. 6). The high precision and accuracy of the current instrument allows the analysis of complex multicomponent samples, yielding accurate and independent determination of preexponential factors (thermodynamics) and lifetimes (structural dynamics) (Fig. 7). We have recently used this instrument to measure not only several lifetimes, but several Gaussian distributions of lifetimes, demonstrating the exceptional precision and linearity of the instrument.[17,18]

B. Comparison with TCSPC

A single-pulse HPTRF experiment on a micromolar sample can achieve $S/N \sim 100$, and this can be repeated every 0.1 ms (Figs. 2 and 4). As discussed in Introduction and demonstrated in Fig. 4, the equivalent S/N requires 60 s in an optimized TCSPC experiment, so HPTRF produces a factor of 6×10^5 increase in throughput, with no sacrifice in accuracy or precision. This suggests that the number of photons detected in the HPTRF experiment from a single pulse must be $\sim 6 \times 10^6$, as in the entire 60 s TCSPC experiment. This hypothesis can be tested by calculating the number of photons detected in a single HPTRF experiment, based on the integrated signal intensity and the voltage applied to the PMT (Ref. 3)

$$C = I/R,$$
$$P = C/(G \times 1.6 \times 10^{-19}\ \text{C/electron}), \tag{2}$$

where C (coulombs) is the total PMT output charge, corresponding to the integrated fluorescence waveform I (volt per seconds) divided by the input resistance ($R = 50\ \Omega$), P is the total number of detected photons assuming 1 photon induces 1 electron in the PMT, and G is the PMT amplification gain determined from the PMT voltage according to the manufacturer's specifications. This calculation yields 2×10^5 photons detected in a single pulse for 5 μM anthracene [Fig. 2(a)] and 2×10^6 photons for 1 μM Rh6G [Fig. 2(b)]. These numbers are consistent with the total number of photons emitted from each sample, which, given the excitation pulse energy, sample absorbance and quantum yield, is at least 10^{10} and 10^{11}, respectively. Thus HPTRF is able to achieve a high degree of precision and accuracy because $>10^5$ emitted photons can be detected per laser pulse. Advances in PMT and digitizer linearity have made this approach tractable, yielding results at least as accurate as TCSPC in a tiny fraction of the time (Fig. 4). Thus "high performance" designates this instrument's unique combination of high-throughput and accuracy.

TCSPC has been the method of choice for the analysis of fluorescence lifetimes for four decades, but it is fundamentally incapable of high throughput with high S/N. Since both instruments are now available in our laboratory, are there cases where TCSPC is preferred to HPTRF? In principle, TCSPC might have superior time resolution, since the IRF and acquisition channel width of HPTRF are wider by factors of 3 and 2, respectively. However, this apparent advantage of TCSPC is not confirmed by the results, since HPTRF yields accurate lifetimes as short as 100 ps (Table I, Fig. 6). This is probably because the longer IRF and channel widths of HPTRF are compensated by increased uniformity. Further studies directly comparing the two instruments will be needed to determine whether TCSPC is superior for measuring extremely short lifetimes, but the present result suggest that HPTRF is at least as accurate for lifetimes well below 1 ns. The only cases in which TCSPC is preferred over HPTRF in our own laboratory are those in which (a) the desired excitation wavelength is available in a diode laser but not in a microchip laser or (b) the fluorescent signal is so weak that it is not feasible to detect multiple emitted photons per excitation pulse. TCSPC remains the preferred method for extremely weak signals.

While the TCSPC approach has already reached its theoretical maximum in throughput, future enhancements in the throughput of HPTRF are quite feasible. Our current pulse repetition rate of 10 kHz is 1000 times slower than the optimal rate for a 10 ns lifetime signal. As lasers with higher repetition frequencies become available, along with digitizers capable of keeping up with the data stream, it should be possible to improve throughput into the submicrosecond range with HPTRF.

C. Potential future applications

HPTRF makes possible several new classes of applications. If this system is coupled to a rapid mixing device, it can measure transient changes in time-resolved fluorescence waveforms following mixing of two samples, with 0.1 ms kinetic resolution. Each waveform can contain detailed structural information (e.g., resonance energy transfer within an enzyme), and the submillisecond time-dependence of the detected waveforms can connect structural dynamics directly with the kinetic mechanism. Alternatively, HPTRF could be coupled to a relaxation-jump device (pressure or temperature).[18] It could also be implemented within a microplate reader and used for high-throughput sample screening assays or in a microscope or flow cytometer for high-throughput analysis of time-resolved fluorescence in cells.

ACKNOWLEDGMENTS

Instrumentation and software at University of Minnesota were primarily the work of Igor Negrashov. This research was supported by NIH grants to D.D.T. (Contract Nos. AR032961 and GM027906), J.M.M. (Contract No. F32AR056191), A.S.L. (Contract No. GM069783), and by grants from the Montana Board of Research and Commercialization Technology to G.D.G. (Grant Nos. 08-48 and 10-75).

[1] J. R. Lakowicz, *Principles of Fluorescence Spectroscopy*, 3rd ed. (Springer, New York, 2006), Chap. 4.
[2] M. Köllner and J. Wulfrum, Chem. Phys. Lett. **200**, 199 (1992).
[3] L. P. Hart and M. Daniels, Appl. Spectrosc. **46**, 191 (1992).
[4] J. R. Taylor, M. C. Adams, and W. Sibbett, Appl. Phys. (Berlin) **21**, 13 (1980).

[5] S. A. Nowak, F. Basile, F. E. Kivi, and F. E. Lytle, Appl. Spectrosc. **45**, 1026 (1991).
[6] T. L. Campos and F. E. Lytle, Appl. Spectrosc. **46**, 1859 (1992).
[7] E. H. Ellison and J. K. Thomas, J. Phys. Chem. B **105**, 2757 (2001).
[8] Z. S. Kolber and M. D. Barkley, Anal. Biochem. **152**, 6 (1986).
[9] Y. O. Posokhov and A. S. Ladokhin, Anal. Biochem. **348**, 87 (2006).
[10] J. M. Beechem, M. Ameloot, and L. Brand, Chem. Phys. Lett. **120**, 466 (1985); J. M. Beechem, Chem. Phys. Lipids **50**, 237 (1989); Methods Enzymol. **210**, 37 (1992).
[11] J. R. Knutson, J. M. Beechem, and L. Brand, Chem. Phys. Lett. **102**, 501 (1983).
[12] A. Grinvald, Anal. Biochem. **75**, 260 (1976).
[13] M. Tanaka, F. Tanaka, S. Tai, K. Hamanoue, M. Sumitani, and K. Yoshihara, J. Phys. Chem. **87**, 813 (1983).
[14] D. Magde, G. E. Rojas, and P. G. Seybold, Photochem. Photobiol. **70**, 737 (1999).
[15] N. Boens, W. Qin, N. Basaric, J. Hofkens, M. Ameloot, J. Pouget, J. P. Lefevre, B. Valeur, E. Gratton, M. vandeVen, N. D. Silva, Jr., Y. Engelborghs, K. Willaert, A. Sillen, G. Rumbles, D. Phillips, A. J. Visser, A. van Hoek, J. R. Lakowicz, H. Malak, I. Gryczynski, A. G. Szabo, D. T. Krajcarski, N. Tamai, and A. Miura, Anal. Chem. **79**, 2137 (2007).
[16] L. E. Cramer and K. G. Spears, J. Am. Chem. Soc. **100**, 221 (1978).
[17] R. V. Agafonov, I. V. Negrashov, Y. V. Tkachev, S. E. Blakely, M. A. Titus, D. D. Thomas, and Y. E. Nesmelov, Proc. Natl. Acad. Sci. U.S.A. **106**, 21625 (2009).
[18] D. Kast, M. Espinoza-Fonseca, C. Yi, and D. Thomas, Proc. Natl. Acad. Sci. U.S.A. **107**, 8207 (2010).